Physicochem. Probl. Miner. Process., 54(2), 2018, 355-362

http://www.journalssystem.com/ppmp

Physicochemical Problems of Mineral Processing

ISSN 1643-1049

Received May 2, 2017; reviewed; accepted July 18, 2017

Bubble loading profiles in a flotation column

Amir Eskanlou, Mohammad Reza Khalesi, Mahmoud Abdollahy

Mining Engineering Department, Tarbiat Modares University, Tehran, Iran

Corresponding author: mrkhalesi@modares.ac.ir (Mohammad Reza Khalesi)

Abstract: Bubble loading is the mass of hydrophobic particles attached per unit surface area of air. This measure can be used in the design and analysis of flotation columns as a sign of true flotation. To date, however, this measurement has been limited to the pulp-froth interface, which only indicates the maximum bubble loading and does not reflect the progress of the loading process. This paper introduces the concept of bubble loading profile that summarizes measures of bubble loading at different heights of the collection zone in a flotation column. The effects of bubble size, particle size and collector dosage on the introduced profiles are also investigated. These operational variables changed the bubble loading profile from a linear to a curved trend. The curvatures in the profiles were near the place of the feeding port and therefore the collection zone was divided into two separate zones in terms of bubble loading characteristics. The zone below the feeding port often did not contribute much to the loading of particles on the bubbles and the loading phenomenon mostly took place above the feeding port. Behaviors of the profiles in these two zones were analyzed to reveal that a change in the feeding port placement or column height can, under some conditions, increase the overall bubble loading and thus, ultimately, the true flotation.

Keywords: *bubble loading, flotation column, profile, collection zone height*

1. Introduction

Flotation is a separation process that exploits the differences in the superficial properties of particles to separate the valuable from the gangue minerals (Wills and Finch, 2016). Particle-bubble interactions and consequently the mass loading of bubbles is a key to understanding of froth flotation (Nguyen et al., 2003). The mass of hydrophobic particles attached per unit surface of air bubbles in the pulp phase of a flotation cell is referred to as the bubble loading (Bradshaw and O'Connor, 1996) and as a macroscopic measure; it represents the true flotation (Yianatos et al., 2015). The knowledge of particle loading on bubbles in the pulp phase of a flotation cell is very important in understanding the sub-processes of the collection zone (Bradshaw and O'Connor, 1996). The collection zone in a flotation column dictates the vessel dimensions, as the column height is most influenced by the collection zone height (Yianatos et al., 1988). In order to incorporate bubble loading into the study of collection zone, it is imperative to study this measure in different parts of the zone. However, so far, investigations on bubble loading have been limited to maximum bubble loading measured in the pulp-froth interface (King, 1974; Falutsu and Dobby, 1992; Dyer, 1995; Bradshaw and O'Connor, 1996; Uribe-Salas et al., 2003; Seaman et al., 2004; Barbian et al., 2007; Moys et al., 2010; Hemmati-Chegeni et al., 2016) and the evolution of the bubble loading process is unknown. This paper aims to study the bubble loading in different positions of the collection zone from the bubble generator to the pulp-froth interface in a flotation column and introduces this analysis as the bubble loading profile. The bubble loading profile delineates the mass loading behavior of air bubbles during their journey within the collection zone. This concept introduces a new set of zones within a flotation column based on their contribution to the overall bubble loading efficiency. Further, the effect of three operating variables (bubble size, particle size and collector dosage) on the bubble loading profile are investigated. These variables were chosen due to their importance in the flotation process. Bubble and particle sizes are physical variables that

http://dx.doi.org/10.5277/ppmp1819

are intimately linked to the bubble-particle collision (Ahmed et al., 1985). The importance of bubble size and its effect on the flotation sub-processes has been discussed extensively in the literature (Hassanzadeh et al., 2016; Kouachi et al., 2015 & 2017). The collector dosage, as a chemical variable, dictates the surface characteristics of solid particles and thereupon influences the attachment and detachment sub-processes (Rahman et al., 2012).

2. Experimental

The flotation column used in this research was a laboratory column (5.4 cm diam. × 116 cm height) with laminar flow regime and least mixing, designed by Hemmati-Chegeni et al. (2015). The experimental procedure, including the bubble loading measurements, generation of a narrow bubble size distribution (BSD) and measurement of the BSD were performed using the methodology and apparatus found in Hemmati-Chegeni et al. (2016). Equipment with similar principle of operation has already been described in the literature (Malysa et al., 1999; Grau and Heiskanen, 2002; Rodrigues and Rubio, 2003). The BSD was analyzed using the codes developed in image processing toolbox of MATLAB®. Images were acquired by a digital camera (Dino-Lite Digital Microscope AM-7013M) using a HUT bubble analyzer in accordance with Mazahernasab and Ahmadi, (2016), as shown in Fig. 1. According to the results of the BSD analysis, 0.8 and 1.8 mm were the means of the two BSDs with standard deviations of 0.15 and 0.2 mm, respectively. As well, no remarkable change of BSD in different heights of the column was observed. In order to determine the bubble loading profile, the bubble sampler used by Hemmati-Chegeni et al. (2016) was redesigned and reconstructed to allow sampling of the air bubbles from different heights of the collection zone. Thus, the new sampling apparatus consisted of a riser tube (15 mm internal diam. × 720-1520 mm variable length) and a collection chamber (50 mm diam. × 150 mm height) made of transparent Perspex, as shown in Fig. 2-a. Fig. 2-b shows the sampler installed above the column. Pure quartz (99.64%, 2.65 g/cm^3) was used to prepare the flotation pulp; the XRF analysis of the mineral is presented in Table 1. In the present study, the quartz samples were cleaned by washing in a solution composed of 2.5% H_2SO_4 (by volume) and 2.5% NaOH (by weight) and then rinsed with de-ionized water to ensure that the particles were free of any contamination and their surface were hydrophilic in accordance with Gungoren et al. (2017). The samples were then left to dry in clean room environment. To investigate the effects of the operating variables on the bubble loading profile, two bubble sizes (0.8 and 1.8 mm) and three particle sizes (63–106, 106–150 and 150–300 μm) were tested in three collector dosages (50, 100 and 150 g/Mg). The values of these variables were based on previous studies and preliminary tests, to ensure that the effects of selected physical and chemical variables would be observable on the bubble loading profile. Dodecylammonium chloride (0.5 g/dm^3 dodecylamine solution in HCl at pH = 3) and A65 (polypropylene glycol) were the collector and frother reagents, respectively. Any pH adjustments were conducted using sodium hydroxide (NaOH). A summary of the experimental conditions is presented in Table 2, and a schematic diagram of the experimental setup is shown in Fig. 3. To determine the bubble loading profile using the newly designed sampling apparatus, air bubbles were sampled from five different heights of the collection zone (i.e., 20, 40, 60, 80 and 100 cm) and bubble loading was measured for each targeted height of the zone in separate flotation runs. In order to measure the bubble loading in a specific height, first of all, the aeration system (sparger) at the bottom of the column was opened, and then the column was filled with the frother-water mixture (prepared earlier), to prevent bubble coalescence within the column and also to get the column ready for the next steps. Then, the nozzle at the bottom of the riser tube of the sampler was closed with a bung, and then the sampler was inserted into the flotation cell so that the nozzle was located at the target height in the collection zone where the sampler was fixed. Later on, the sampler was also filled with the frother–water mixture to prevent bubbles from coalescing during sampling. Afterwards, the upper orifice of the sampler was closed with a bung as well. Outside the column, the pulp was conditioned with the cationic collector for 10 min and then was fed into the column with a feeding rate of 0.847 dm^3/min for 60 s until the column was completely filled with the slurry. Then, the bung was removed from the bottom of the riser to let the floated bubbles (loaded and unloaded) enter the collection chamber through the riser tube for about 120 s. Upon reaching the collection chamber, the bubbles burst at the liquid/gas interface in the chamber and the particles were detached. Detached

particles then settled to the lower part of the chamber, while the air volume accumulated in the upper part of the chamber. Displaced water–frother solution equivalent to the total volume of the accumulated bubbles, exited the chamber through the outlet #2 (see Fig. 3) based on the positive displacement principle with the help of a peristaltic pump and then passed through the filter to capture any suspended solid particles preventing them entering the flotation cell. The displaced water was then recycled to the riser tube through the displaced water entrance as shown in Fig. 3. The countercurrent flow of the displaced water within the riser tube helped prevent any possible entrained particles to enter the collection chamber. The bias velocity of the displaced water in the riser tube was adjusted via pump speed where a bias velocity of less than or equal to the superficial gas velocity was maintained in order to prevent loaded particles being detached from aggregates in the riser tube, as well as allowing entrained particles to return back down to the cell. At the end of the experiment, the tailing outlet (discharge valve) of the column was opened immediately to drain all the pulp out of the column where at the same time the suction rate of the peristaltic pump was increased until the remaining water in the collection chamber was completely drained and passed through the filter to ensure that no loss of sample occurs. The time of sampling was recorded along with the volume of water displaced (volume of air accumulated) and the mass of particles trapped in the device as well as in the filter. The collected particles were then dried and weighed and then using the calculation procedure presented by Hemmati-Chegeni et al. (2016), bubble loading was quantified. As there was a short distance from the feeding port to the pulp-froth interface (see Fig. 3), only one target height (i.e., 100 cm) was selected above the feeding port for bubble loading measurements. Similar to all previous studies on bubble loading (except for the single bubble investigations), the measured bubble loading in this study indicates the "mean" mass of solid particles attached per unit surface of air bubbles, as the captured bubbles may be loaded with different number of particles. Besides, due to the design of the experimental set up, no entrainment of unattached particles was possible in flotation runs (as explained by Hemmati-Chegeni et al. (2016)). Finally, in order to check the reproducibility of the results, measurements were randomly selected and repeated, where results showed a discrepancy of less than five percent.

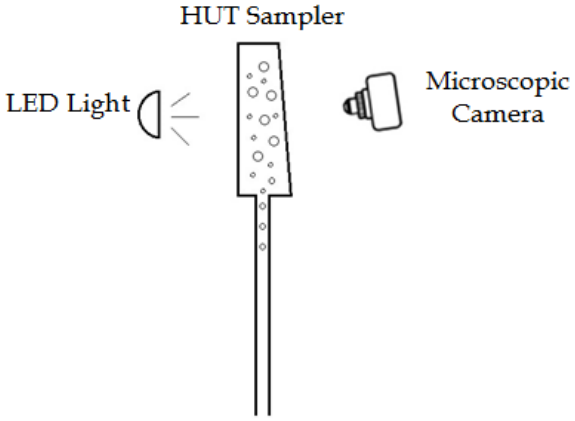

Fig. 1. Image acquisition apparatus for bubble size distribution analysis

Table 1. Results of the XRF analysis

Composition	%	Composition	%
P_2O_5	0.005	SiO_2	99.64
TiO_2	0.011	Al_2O_3	0.05
MnO	0.001	Fe_2O_3	0.31
L.O.I	0.03	CaO	0.06
Ba (ppm)	24	Na_2O	0.01
Cl (ppm)	15	MgO	0.01
S (ppm)	7	K_2O	0.01

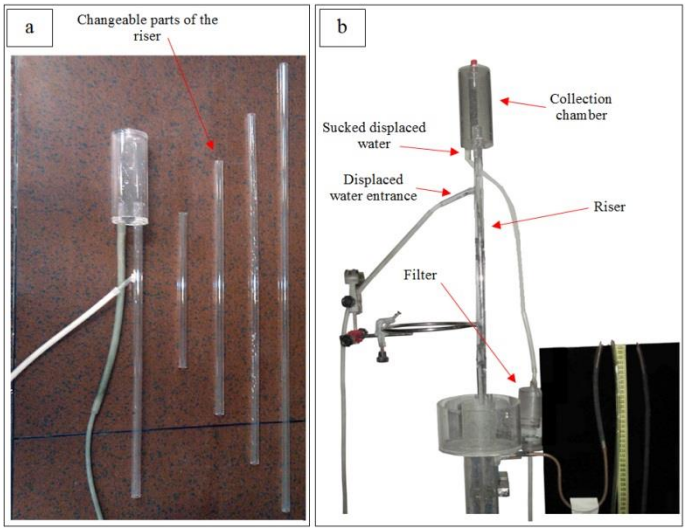

Fig. 2. a- Loaded bubbles sampling apparatus including riser with changeable parts and collection chamber, b- placement of sampler on top of the column

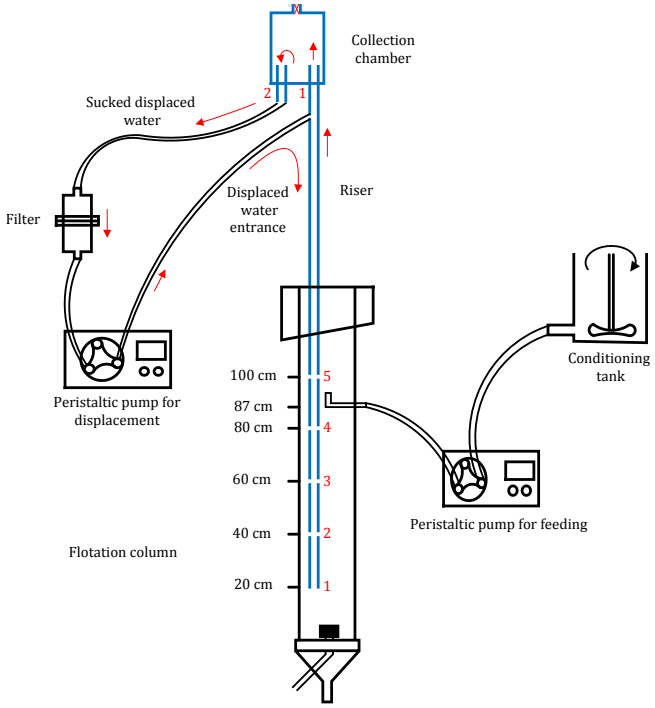

Fig. 3. Schematic diagram of the apparatus used for the determination of bubble loading profiles

Table 2. Experimental conditions for bubble loading measurements

Feeding rate (cm^3/min)	847	Feed solid weight (g)	300
Aeration rate (cm^3/min)	300	Feed solid content (%)	10
Bubble sizes (mm)	0.8, 1.8	Collector dosage (g/Mg)	50, 100, 150
Frother dosage for small bubbles (ppm)	45	Pulp conditioning time (min)	10
Frother dosage for large bubbles (ppm)	30	pH	7
Frother conditioning time (min)	10	Impeller speed in pulp conditioning (rpm)	250
Dodecylamine (g/dm^3)	0.5	Number of sampling points in collection zone	5

2. Results and discussion

Bubble loading profiles were determined in the flotation column for different operational conditions and results are presented in Fig. 4. The bubble loading profile was linear (with a constant slope) when bubble size, particle size and collector dosage were 0.8 mm, 63-106 μm and 50 g/Mg, respectively (Fig 4-a). The linearity of the bubble loading profile in a flotation column implies that the efficient collection zone height for flotation of solid particles extends to the whole distance from the sparger to pulp-froth interface. In addition, a linear profile for bubble loading indicates that the mass loading rate of air bubbles along the collection zone was constant. Thus, greater collection zone height will result in higher bubble loading values, i.e., an increase in the column height is favorable in terms of bubble loading. Therefore, for this particle and bubble size, if 50 g/Mg of collector is used, increasing the column height could facilitate increased recovery of attached particles. When the collector dosage was increased to 100 g/Mg, the profile showed a distinct curvature, where the slope of the variation in bubble loading vs. height of the column changed at a height of 60 cm. This curvature became more pronounced when the collector dosage increased to 150 g/Mg. In that case, the zone in which bubble loading takes place was limited to a specific section near the feeding port of the cell up to the pulp-froth interface. Increase of pulp concentration near the feed inlet is reported by Finch and Dobby, (1990), which could be a reason for different behavior of bubble loading in this zone. Thus, for this collector dosage, changing the place of the feeding port is more important than increasing the column height, as the effective area of bubble loading was limited to the section above the feeding port. This was experimentally reported by Patil et al. (2010) who found that changing the feed inlet height in the column flotation of coal enhances the flotation performance and product yield. Results of this paper link their finding to bubble loading phenomenon.

As the bubble size increased from 0.8 to 1.8 mm, the bubble loading profile kept its linear behavior in all the three collector dosages (Fig. 4-b). In other words, larger values of maximum bubble loading attained with 1.8 mm bubbles in Fig. 4-b, compared to the results of Fig 4-a, could be attributed to the fact that with small bubbles, the zone below the feeding port did not contribute to bubble loading, while in case of coarser bubbles, loading of bubbles initiated from the point just above the sparger and thus the full height of the collection zone contributed to the bubble loading process.

For the particle size of 106-150 μm in the presence of small bubbles (0.8 mm), bubble loading took place only in a specific zone from feeding port to the interface, showing approximately the same profiles for all collector concentrations (Fig. 4-c). Particle collection efficiency was poor in the zone below the feeding port (from the sparger to the height of 60 cm, in this case), and this part of the collection zone had a poor contribution to the overall flotation efficiency. Fig. 4-d indicates that the bubble loading profile reaches a plateau near the pulp-froth interface using collector dosages of 50 and 100 g/Mg, which indicates that under such conditions, an increase in column height is unlikely to add to the overall loading of bubbles.

For the particle size of 150-300 μm, a remarkable drop was observed in bubble loading values compared to the smaller particle sizes, and this was greatest for small bubbles, as shown in Figs. 4-e & f. Loading of coarse particles on bubbles was significant only when large bubbles and high collector dosage were applied. In this case, it seems that increasing the collection zone above the feeding port could improve the collection efficiency. Selection of an optimum collection zone height in flotation columns according to the operational requirements has already been discussed by several researchers (Yianatos et al., 1988; Ityokumbul, 1992; Ityokumbul, 1993; Garibay et al., 2002), among which Ityokumbul, (1993) discussed a new approach to flotation column design based on the consideration of bubble loading rate where the flotation process was considered to be analogous to the interface mass transfer. Flint and Burstein, (2000) also described bubble loading along with retention time, mixing characteristics and maximum gas rate as main design criteria for collection zone in flotation columns. In addition to the findings of the previous researchers, the present study mainly highlights the role of bubble loading vertical profile in the design and optimization of flotation columns.

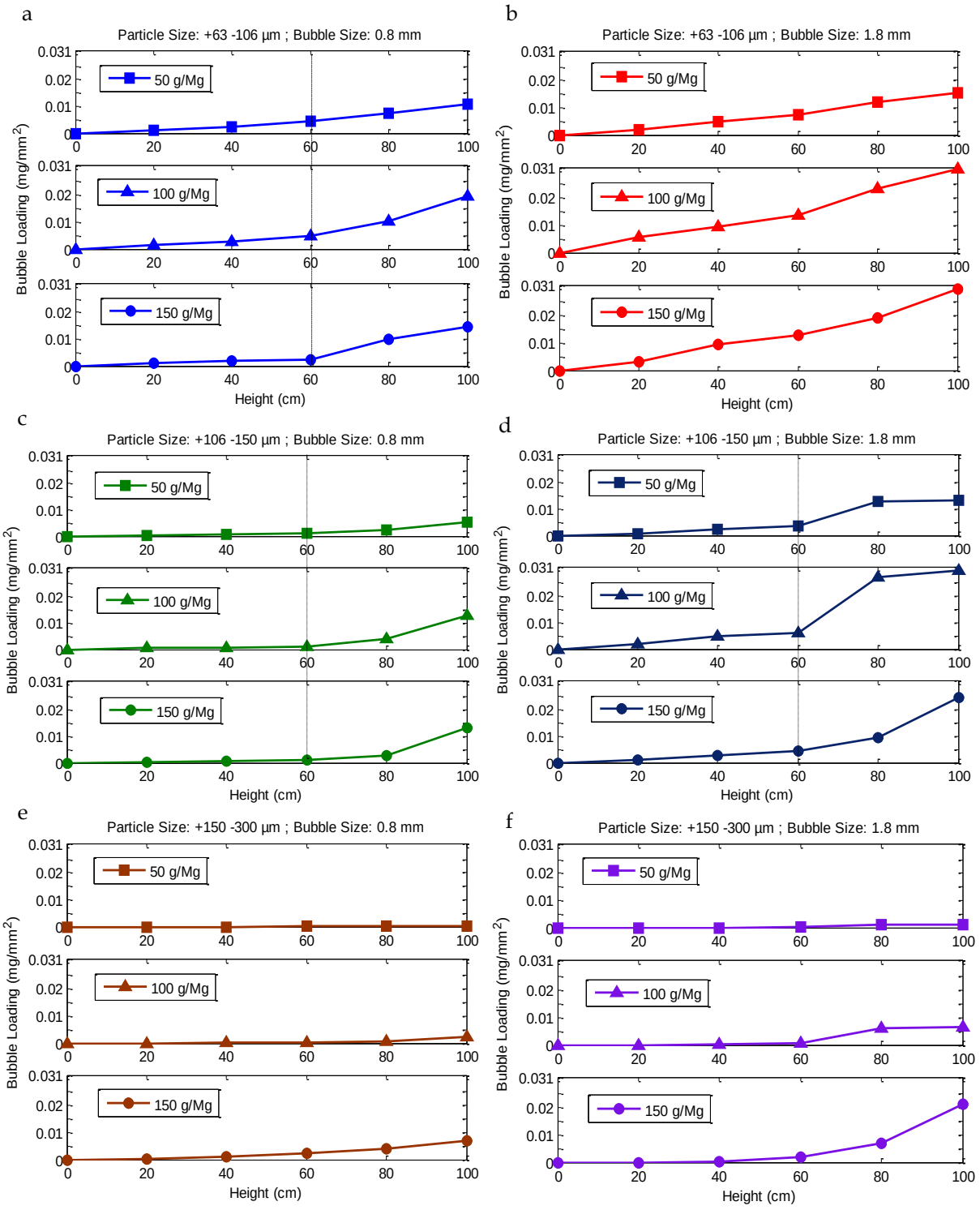

Fig. 4. Bubble loading profiles for particle size fractions of +63-106, +106-150 & +150-300 µm using collector dosages of 50, 100 and 150 g/Mg. Right: Bubble size of 0.8 mm; Left: Bubble size of 1.8 mm

3. Conclusions

The bubble loading vertical profile, which measures bubble loading at different heights of a laboratory column flotation cell, is introduced in this paper. Measurements were taken under different operational conditions to investigate the effect of parameters on the loading profile. Both the absolute values of bubble loadings and the profiles depended on the operational conditions. An interesting observation, common to many profiles, was that the zone below the feeding port often did not

contribute much to the loading of particles on the bubbles and that the loading phenomenon mostly took place above the feeding port. Therefore, in terms of bubble loading phenomenon, the collection zone could be divided into two separate zones below and above the feeding port, each of which showed different mass loading characteristics. It was also observed in many cases that bubble loading tended to increase while ascending and therefore an increase of column height could increase total bubble loading. Such observations have potential application in the design of columns with respect to height and the placement of the feeding port. Furthermore, in some cases, the addition of more collector reagents could be replaced by a change in the column design, i.e., a better design of the column regarding the height and the placement of the feeding port can reduce reagent usages. The concept of the bubble loading profile is also well-suited for modeling flotation kinetics based on bubble loading, which is the current work of this research team.

References

AHMED, N., JAMESON, G.J., 1985. *The effect of bubble size on the rate of flotation of fine particles.* International Journal of Mineral Processing, 14(3), 195-215.

BARBIAN, N., CILLIERS, J.J., MORAR, S.H., BRADSHAW, D.J., 2007. *Froth imaging, air recovery and bubble loading to describe flotation bank performance.* International Journal of Mineral Processing, 84(1), 81-88.

BRADSHAW, D.J., O'CONNOR, C.T., 1996. *Measurement of the sub-process of bubble loading in flotation.* Minerals Engineering, 9(4), 443-448.

DYER, C., 1995. *An Investigation into the Properties of the Froth Phase in the Flotation Process.* University of the Witwatersrand.

FALUTSU, M., DOBBY, G.S., 1992. *Froth performance in commercial sized flotation columns.* Minerals Engineering, 5(10-12), 1207-1223.

FINCH, J.A., DOBBY, G.S., 1990. *Column Flotation.* Pergamon Oxford.

HEMMATI-CHEGENI, M., ABDOLLAHY, M., KHALESI, M.R., 2015. *Column flotation cell design by drift flux and axial dispersion models.* International Journal of Mineral Processing, 145, 83-86.

HEMMATI-CHEGENI, M., ABDOLLAHY, M., KHALESI, M.R., 2016. *Bubble loading measurement in a continuous flotation column.* Minerals Engineering, 85, 49-54.

HASSANZADEH, A., HASSAS, B.V., KOUACHI, S., BRABCOVA, Z., CELIK, M.S., 2016. *Effect of bubble size and velocity on collision efficiency in chalcopyrite flotation.* Colloids and Surfaces A: Physicochemical and Engineering Aspects, 498, 258-267.

ITYOKUMBUL, M.T., 1992. *A mass transfer approach to flotation column design.* Chemical engineering science, 47(13), 3605-3612.

ITYOKUMBUL, M.T., 1993. *Selection of recovery zone height in flotation column design.* Chemical Engineering and Processing: Process Intensification, 32(2), 77-82.

GUNGOREN, C., OZDEMIR, O., OZKAN, S.G., 2017. *Effects of temperature during ultrasonic conditioning in quartz-amine flotation.* Physicochemical Problems of Mineral Processing, 53(2), 687-698.

GARIBAY, R.P., 2002. *Effect of collection zone height and operating variables on recovery of overload flotation columns.* Minerals Engineering, 15(5), 325-331.

GRAU, R.A., HEISKANEN, K., 2002. *Visual technique for measuring bubble size in flotation machines.* Minerals Engineering, 15(7), 507-513.

KING, R.P., HULBERT, D.G., HATTON, T.A., 1974. *Bubble loading during flotation.* Trans. Instn. Min. Metall. Vol C., C112-C115.

KOUACHI, S., HASSANZADEH, A., BOUHENGUEL, M., HASSAS, B.V., ÇELIK, M.S., 2015, *Contribution of interceptional effect to collision efficiency of particle bubble encounter in flotation.* In XVI Balkan Mineral Processing Congress, Belgrade-Serbia, 339-345.

KOUACHI, S., HASSAS, B.V., HASSANZADEH, A., ÇELIK, M.S., BOUHENGUEL, M., 2017. *Effect of negative inertial forces on bubble-particle collision via implementation of Schulze collision efficiency in general flotation rate constant equation.* Colloids and Surfaces A: Physicochemical and Engineering Aspects, 517, 72-83.

MALYSA, K., NG, S., CYMBALISTY, L., CZARNECKI, J., MASLIYAH, J., 1999. *A method of visualization and characterization of aggregate flow inside a separation vessel, Part 1. Size, shape and rise velocity of the aggregates.* International Journal of Mineral Processing, 55(3), 171-188.

MOYS, M.H., YIANATOS, J., LARENAS, J., 2010. *Measurement of particle loading on bubbles in the flotation process.* Minerals Engineering, 23(2), 131-136.

MAZAHERNASAB, R., AHMADI, R., 2016. *Determination of bubble size distribution in a laboratory mechanical flotation cell by a laser diffraction technique.* Physicochemical Problems of Mineral Processing, 52(2), 690-702.

NGUYEN, A.V., NALASKOWSKI, J., MILLER, J.D., 2003. *A study of bubble–particle interaction using atomic force microscopy.* Minerals Engineering, 16(11), 1173-1181.

PATIL, D.P., PAREKH, B.K. AND KLUNDER, E.B., 2010. *A novel approach for improving column flotation of fine and coarse coal.* International Journal of Coal Preparation and Utilization, 30(2-5), 173-188.

SEAMAN, D.R., FRANZIDIS, J.P., MANLAPIG, E.V., 2004. *Bubble load measurement in the pulp zone of industrial flotation machines – a new device for determining the froth recovery of attached particles.* International Journal of Mineral Processing, 74(1), 1-13.

RODRIGUES, R.T., RUBIO, J., 2003. *New basis for measuring the size distribution of bubbles.* Minerals Engineering, 16(8), 757-765.

RAHMAN, R.M., ATA, S., JAMESON, G.J., 2012. *The effect of flotation variables on the recovery of different particle size fractions in the froth and the pulp.* International Journal of Mineral Processing, 106, 70-77.

URIBE-SALAS, A., DE LIRA-GOMEZ, P., PEREZ-GARIBAY, R., NAVA-ALONSO, F., MAGALLANES-HERNANDEZ, L., LARA-VALENZUELA, C., 2003. *Overloading of gas bubbles in column flotation of coarse particles and effect upon recovery.* International Journal of Mineral Processing, 71(1), 167-178.

WILLS, B.A., FINCH, J.A., 2016. *Chapter 12 - Froth Flotation.* Wills' Mineral Processing Technology (Eighth Edition). BosMg: Butterworth-Heinemann.

FLINT, L.M., BURSTEIN, M.A., 2000. *Froth processes and the design of column flotation cells.* Academic Press, 1521-1527.

YIANATOS, J.B., ESPINOSA-GOMEZ, R., FINCH, J.A., LAPLANTE, A.R., DOBBY, G.S., 1988. *Effect of column height on flotation column performance.* Minerals and Metallurgical Process, 11-14.

YIANATOS, J., VINNETT, L., CARRASCO, C., ALVAREZ-SILVA, M., 2015. *Effect of entrainment in bubble load measurement on froth recovery estimation at industrial scale.* Minerals Engineering, 72, 31-35.